Optimal ASV Path-Following for Improved Marine Survey Data Quality

Kleio Baxevani, Grantt E. Otto, Arthur C. Trembanis and Herbert G. Tanner

***Abstract*—Marine geophysical surveys are one of the methods utilized to map the seabed or water column for a variety of use cases. Multibeam echosounders (MBES), sidescan sonar (SSS), and subbottom profilers (SBP) are examples of instruments used to accurately quantify or georeference seafloor characteristics for applications such as navigation safety/keel clearance, offshore wind or coastal scientific studies. Autonomous vehicles can collect similar quality data to that collected by a large vessel at a fraction of the cost and human involvement and with a much smaller carbon footprint. This paper builds upon previous work [1] and proposes a new path-following control approach for an autonomous surface vehicle (ASV) using a more realistic kinematics model that includes lateral drift. The performance of the new controller is verified through simulations and field testing showcasing the improvement in the vessel's motion and the acquired sonar data.**

***Index Terms*—Autonomous Surface Vehicles, Marine Robotics, Hydrographic Surveys**

I. Introduction

Spanning a wide range of applications, from updating navigational charts to implementing offshore energy solutions, the use of marine geophysical data products such as multibeam sonar grids or sidescan sonar mosaics can significantly influence critical project decisions. In this context, autonomous marine vehicles can contribute by reducing the cost and accelerating the rate of data collection.

The increasingly stricter requirements across industries for data quality as well as sustainability and reduced carbon footprint motivate the improvement of data collection methods from the sensor to the vessel operation. One of the leading factors in data quality degradation for virtually any hull-mounted marine geophysical surveys is the motion of the vessel itself [2].

In this context, optimizing autonomous surface vehicle (ASV) performance translates to producing smooth motion and reducing disturbances to heading and speed caused by waves or wind. Motion controller improvement represents a cost- and labor-efficient strategy —compared to vehicle design or structure— for reducing some types of motion disturbances. It is also more sustainable as a method because it can be further developed through software updates as opposed to mechanical redesign and fabrication.

The problem this paper addresses is to design and implement an advanced ASV motion control that takes into account platform kinematics and environmental disturbances, with the objective being to improve the field performance of the sensor platform in terms of the quality of the acquired data.

This work is funded by NOAA's Project ABLE.

The authors are affiliated with the Center of Autonomous and Robotic Systems at the University of Delaware. Baxevani and Tanner are with the Mechanical Engineering Department, while Otto and Trembanis are with the School of Marine Science and Policy.

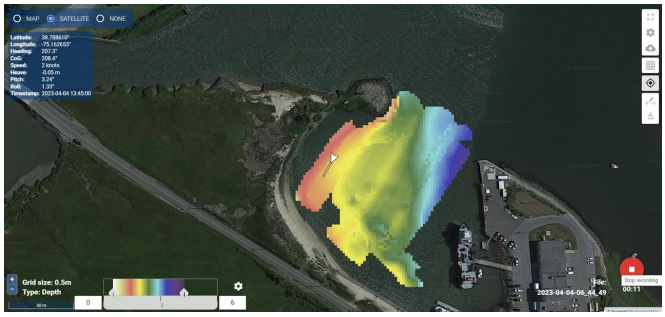

Fig. 1: Screenshot of the software tool utilized to acquire sonar data from University of Delaware boat basin using optimal ASV path-following controller.

Most of the marine vessels used in those applications are underactuated —out of the three degrees of freedom (DOF) they have (surge, sway, yaw) only two are directly controlled (typically, surge and yaw). There is important earlier work on the development of path-following controllers which has leveraged several control design methods, including backstepping [3], [4], sliding mode control [5], [6], model predictive control [7], and fuzzy logic control [8]. While high-accuracy tracking can be achieved with such methods, little attention is usually being paid to the impact of vehicle controlled actuation on the quality of the data the autonomous platform is used to collect. For sidescan sonar data, this quality is affected by sensor platform accelerations, which are not usually directly regulated for data quality purposes. In this application context, reducing or ideally eliminating any oscillations of the sensor system and maintaining a constant forward speed is arguably more important than accurate path tracking during mapping surveys. This work directly addresses this gap.

The main contribution of this work is the design of a novel path-following controller for ASVs conducting marine geophysical surveys, and its testing on the field. This technology applies to both hull-mounted multibeam surveys, where artifacts from excessive vessel motion can be accurately measured and removed, and other instrumentation such as sidescan sonar, where motion artifacts are permanent. The novel path-following controller meets the challenge of balancing accurate trajectory tracking (survey efficiency) against reduction in vehicle accelerations (high-quality data collection), both of which are critical for mission success and commercial viability.

By extending recent results in this direction [1], this paper makes the analysis consistent with SNAME notation, adopts

a more realistic ASV kinematic model that includes drifting terms, redesigns the optimal path following controller to explicitly incorporate and compensate for sway disturbances, provides details on the implementation of the control design on the existing ASV's navigation and control infrastructure, and tests the control design in real sea state conditions.

The rest of the paper is organised as follows. Initially, a brief overview of the system architecture is provided in Section II followed by Section III which introduces the mathematical description of the vehicle and sensor payload kinematics along with the main technical results of the paper. In Section IV the performance of the controller is evaluated numerically through simulations and after laying out the hardware and software tools employed for this integration, the section closes with the field testing results. Finally, Section V concludes the paper with a short overview while also highlighting the potential impact of the approach on the marine robotics industry.

II. Overview of the System

The computational architecture leveraged for this work is part of the Project11 backseat driver,[1] which is an operational graphical user interface and simulator, combined with vessel motion control tools, such as path following and planning, built within the robot operating system (ROS) framework [9]. An overview of the subsystems of interest is illustrated in Fig. 2. The colored-coded boxes indicate different subsystems of the system architecture and the arrows show the information flow among them.

The blue block contains the modules of the motion planning and control system. It runs onboard the vessel and it is responsible for executing the mission plan designed by the operator via the graphical interface (green block). This mission plan is received by the navigation subsystem as a set of waypoints and produces a concatenation of Dubins' vehicle paths to complete the task.

This paper focuses on improving the path-following module of this subsystem, but the proposed control strategy bypasses waypoint navigation with direct vehicle speed feedback control. Once the waypoints defining the survey path are received, the path follower estimates the bearing and the cross-track error between the current position of the vessel (provided by the INS sensor —red block) and the path trajectory. Based on this information, our method generates the desired linear and angular accelerations of the vessel which are then, numerically integrated to produce the linear and angular reference velocities, which are subsequently implemented by the ASV's low-level controller.

The data collection system is represented by the red block. It consists of the sonar acquisition system and the INS sensor which provided the geopose information of the ASV to the whole architecture. This subsystem also runs onboard and stores the sonar and geopose data locally for post-processing purposes.

[1]https://github.com/CCOMJHC/project11

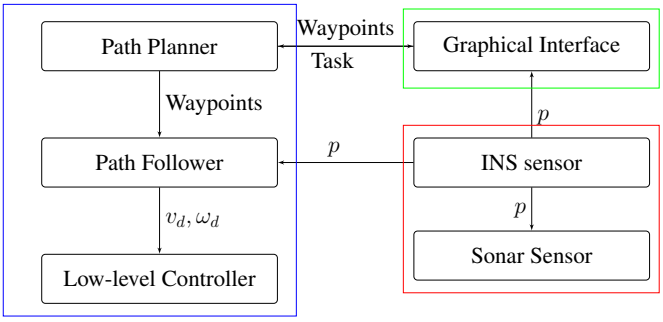

Fig. 2: Block diagram of the system architecture. *Blue*: The motion planning and control of the vessel takes place onboard using geopose information provided by the INS sensor. *Green*: The graphical user interface runs on a ground station desktop on-shore. *Red*: The sonar acquisition system records and stores data onboard using geopose information provided by the INS sensor.

III. Optimal Path-Following Controller

Consider an ASV with three DOFs kinematics, for surge, sway and yaw. The generalized positions and velocities can be defined as $\boldsymbol{\eta} = [x, y, \psi]^\intercal$ and $\boldsymbol{\nu} = [u, v, r]^\intercal$, respectively. Thus, the matrix-vector representation of the craft's kinematics [10] can take the form

$$\dot{\boldsymbol{\eta}} = \boldsymbol{R}(\psi)\boldsymbol{\nu} \text{ where } \boldsymbol{R}(\psi) = \begin{bmatrix} \cos\psi & -\sin\psi & 0 \\ \sin\psi & \cos\psi & 0 \\ 0 & 0 & 1 \end{bmatrix} . \quad (1)$$

The goal is to control the ASV so that it conducts a lawnmower pattern survey over an area of interest, in a way that ensures the collection of high-quality sidescan sonar data. The approach adopted to achieve survey path following performance *with* high-quality data collection, is by minimizing the accelerations induced at the sensor payload location.

Let $\boldsymbol{\eta_s} = [x_s, y_s, \psi_s]^\intercal$ denote the coordinates of the ASV's sensor payload (s for sensor), assuming that the sensor is placed somewhere along the longitudinal axis of symmetry of the vehicle and at a distance δ from the midpoint between the two propellers. In our case this is a translational change of coordinates which implies that the yaw remains the same. The new position vector is expressed with respect to $\boldsymbol{\eta}$ as

$$x_s = x + \delta\cos\psi \quad (2a)$$
$$y_s = y + \delta\sin\psi \quad (2b)$$
$$\psi_s = \psi \ , \quad (2c)$$

and the respective velocities are

$$\dot{x}_s = \dot{x} - \delta\, r\, \sin\psi = u\cos\psi - (v + \delta\, r)\sin\psi \quad (3a)$$
$$\dot{y}_s = \dot{y} + \delta\, r\, \cos\psi = u\sin\psi + (v + \delta\, r)\cos\psi \quad (3b)$$
$$\dot{\psi}_s = r \ . \quad (3c)$$

To minimize cross-track error *and* accelerations we design an optimal controller which can steer the vessel along a desired line segment with a frame $\{\mathcal{F}\}$. The position and velocity vectors of the sensor expressed on the $\{\mathcal{F}\}$ frame

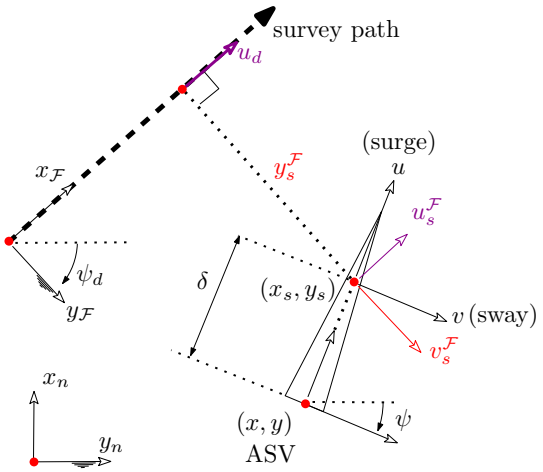

Fig. 3: Illustrative figure defining the different coordinate systems.

are (Fig. 3)

$$\begin{aligned} x_s^{\mathcal{F}} &= o_x^{\mathcal{F}} + x_s \cos\psi_d + y_s \sin\psi_d \\ y_s^{\mathcal{F}} &= o_y^{\mathcal{F}} - x_s \sin\psi_d + y_s \cos\psi_d \end{aligned}$$

$$\begin{aligned} \dot{x}_s^{\mathcal{F}} &= 0 + \dot{x}_s \cos\psi_d + \dot{y}_s \sin\psi_d \\ \dot{y}_s^{\mathcal{F}} &= 0 - \dot{x}_s \sin\psi_d + \dot{y}_s \cos\psi_d \ , \end{aligned}$$

and the acceleration vectors of the sensor on the same frame are derived as

$$\ddot{x}_s^{\mathcal{F}} = \ddot{x}_s \cos\psi_d + \ddot{y}_s \sin\psi_d \tag{4a}$$

$$\ddot{y}_s^{\mathcal{F}} = -\ddot{x}_s \sin\psi_d + \ddot{y}_s \cos\psi_d \ , \tag{4b}$$

where

$$\begin{aligned} \ddot{x}_s &= \dot{u}\cos\psi - u\,r\,\sin\psi - (\dot{v} + \delta\,\dot{r})\sin\psi \\ &\quad - (v + \delta\,r) r \cos\psi \\ \ddot{y}_s &= \dot{u}\sin\psi + u\,r\,\cos\psi + (\dot{v} + \delta\,\dot{r})\cos\psi \\ &\quad - (v + \delta\,r) r \sin\psi \ . \end{aligned}$$

Suppose now that surge acceleration $\dot{u}$ and yaw acceleration $\dot{r}$ are directly controlled through acceleration inputs a_x and α, respectively, and that $\dot{v}$ can be measured as a_y. Renaming

$$a_x \triangleq \dot{u} \quad \alpha \triangleq \dot{r} \quad a_y \triangleq \dot{v} \quad w_x \triangleq \ddot{x}_s^{\mathcal{F}} \quad w_y \triangleq \ddot{y}_s^{\mathcal{F}} \ ,$$

allows one to rewrite the expression of sensor accelerations (3) in matrix form and without time derivative notation as

$$\begin{aligned} \begin{bmatrix} w_x \\ w_y \end{bmatrix} = \begin{bmatrix} \cos\psi_d & \sin\psi_d \\ -\sin\psi_d & \cos\psi_d \end{bmatrix} \Bigg(& \begin{bmatrix} \cos\psi & -\delta\sin\psi \\ \sin\psi & \delta\cos\psi \end{bmatrix} \begin{bmatrix} a_x \\ \alpha \end{bmatrix} \\ & + \begin{bmatrix} -\sin\psi & -\delta\cos\psi \\ \cos\psi & -\delta\sin\psi \end{bmatrix} \begin{bmatrix} u\,r \\ r^2 \end{bmatrix} \\ & + \begin{bmatrix} -\sin\psi \\ \cos\psi \end{bmatrix} a_y + \begin{bmatrix} \cos\psi \\ -\sin\psi \end{bmatrix} v\,r \Bigg) \ , \end{aligned} \tag{5}$$

Given that the sensor accelerations can be directly controlled via a feedback input transformation that maps (3) to an equivalent double integrator system, we can expand the state of (4) as $z = [x_s^{\mathcal{F}}, y_s^{\mathcal{F}}, \dot{x}_s^{\mathcal{F}}, \dot{y}_s^{\mathcal{F}}]^\intercal$ and define a linear system of the following form

$$\begin{bmatrix} \dot{z}_1 \\ \dot{z}_2 \\ \dot{z}_3 \\ \dot{z}_4 \end{bmatrix} = \begin{bmatrix} 0 & 1 & 0 & 0 \\ 0 & 0 & 0 & 1 \\ 0 & 0 & 0 & 0 \\ 0 & 0 & 0 & 0 \end{bmatrix} \begin{bmatrix} z_1 \\ z_2 \\ z_3 \\ z_4 \end{bmatrix} - \begin{bmatrix} 0 & 0 \\ 0 & 0 \\ 1 & 0 \\ 0 & 1 \end{bmatrix} \begin{bmatrix} u_\chi \\ u_\psi \end{bmatrix} \tag{6a}$$

$$\chi = \begin{bmatrix} 0 & 1 & 0 & 0 \end{bmatrix} \begin{bmatrix} z_1 \\ z_2 \\ z_3 \\ z_4 \end{bmatrix} \ . \tag{6b}$$

Based on a well-known result [11] such a linear system has an optimal (steady state) feedback law that would regulate the output $\chi = z_2$ while minimizing the functional

$$J(z, \chi) \coloneqq \int_0^\infty \|z\|^2 + \rho\, w^2 \, \mathrm{d}t \ , \tag{7}$$

for some tunable parameter $\rho > 0$ which expresses the cost of actuation, and which is expressed in terms of a matrix P in the form

$$w_y = -\frac{1}{\rho} \begin{bmatrix} 0 & 1 \end{bmatrix} P \begin{bmatrix} y_s^{\mathcal{F}} \\ \dot{y}_s^{\mathcal{F}} \end{bmatrix} \ , \tag{8}$$

where P is the solution of the algebraic Ricatti equation (ARE) associated with the (lower dimensional compared to (6)) system:

$$\begin{bmatrix} \dot{y}_s^{\mathcal{F}} \\ \ddot{y}_s^{\mathcal{F}} \end{bmatrix} = \begin{bmatrix} 0 & 1 \\ 0 & 0 \end{bmatrix} \begin{bmatrix} y_s^{\mathcal{F}} \\ \dot{y}_s^{\mathcal{F}} \end{bmatrix} - \begin{bmatrix} 0 \\ 1 \end{bmatrix} w_y \tag{9}$$

$$\bar{\chi} = \begin{bmatrix} 0 & 1 \end{bmatrix} \begin{bmatrix} y_s^{\mathcal{F}} \\ \dot{y}_s^{\mathcal{F}} \end{bmatrix} \ . \tag{10}$$

The detailed analytic solution for w_y can then be expressed as:

$$\begin{aligned} w_y &= -\frac{y_s^{\mathcal{F}}}{\sqrt{\rho}} - \frac{\sqrt{2}}{\rho^{1/4}} \Big\{ -[u\cos\psi - (v + \delta\,r)\sin\psi]\sin\psi_d \\ &\quad + [u\sin\psi + (v + \delta\,r)\cos\psi]\cos\psi_d \Big\} \\ &= -\frac{y_s^{\mathcal{F}}}{\sqrt{\rho}} - \frac{\sqrt{2}}{\rho^{1/4}} \big[u\sin(\psi - \psi_d) \\ &\quad + (v + \delta\,r)\cos(\psi - \psi_d)\big] \ . \end{aligned} \tag{11}$$

For the $x_s^{\mathcal{F}}$ dynamics, assume a proportional velocity controller

$$w_x = \tfrac{1}{\rho}(u_d - u) \ , \tag{12}$$

which will regulate the forward speed of the ASV to a desired reference u_d along the path. The choice of the desired speed for the ASV depends on the application, and the type of sensor utilized for the data collection, assuming that we are interested in the sensor data collected along the straight survey lines and not during the transient between them.

Thus, the virtual control inputs are set as (11)-(12) to give exponential convergence to desired surge speed u_d and input optimal regulation of the path tracking error $y_s^{\mathcal{F}}$, and the sensor acceleration form given (5) is equivalent to

$$\begin{bmatrix} a_x \\ \alpha \end{bmatrix} = \begin{bmatrix} \cos\psi & -\delta\sin\psi \\ \sin\psi & \delta\cos\psi \end{bmatrix}^{-1} \Bigg(\begin{bmatrix} \cos\psi_d & \sin\psi_d \\ -\sin\psi_d & \cos\psi_d \end{bmatrix}^{-1} \begin{bmatrix} w_x \\ w_y \end{bmatrix} + \begin{bmatrix} \sin\psi & \delta\cos\psi \\ -\cos\psi & \delta\sin\psi \end{bmatrix} \begin{bmatrix} u\,r \\ r^2 \end{bmatrix} + \begin{bmatrix} \sin\psi \\ -\cos\psi \end{bmatrix} a_y + \begin{bmatrix} -\cos\psi \\ \sin\psi \end{bmatrix} v\,r \Bigg)$$

which is written more compactly as

$$\begin{bmatrix} a_x \\ \alpha \end{bmatrix} = \begin{bmatrix} \cos(\psi_d-\psi) & -\sin(\psi_d-\psi) \\ \frac{1}{\delta}\sin(\psi_d-\psi) & \frac{1}{\delta}\cos(\psi_d-\psi) \end{bmatrix} \begin{bmatrix} w_x \\ w_y \end{bmatrix} + \begin{bmatrix} 0 & \delta \\ -\frac{1}{\delta} & 0 \end{bmatrix} \begin{bmatrix} u\,r \\ r^2 \end{bmatrix} + \begin{bmatrix} 0 \\ -\frac{1}{\delta} \end{bmatrix} a_y + \begin{bmatrix} \sin^2\psi - \cos^2\psi \\ \frac{2}{\delta}\cos\psi\sin\psi \end{bmatrix} v\,r \ . \quad (13)$$

A low-level, discrete-time control design loop then translates the theoretical acceleration inputs into desired velocity commands that can be directly realized on the ASV using its own topside controllers. More specifically, the linear and angular velocity commands at time step k and with step duration Δt can be computed as

$$u_{\text{cmd}}(k) = u(k-1) + \dot{u}(k)\,\Delta t + p_u\big(a(k) - \dot{u}(k)\big)\Delta t^2$$
$$r_{\text{cmd}}(k) = r(k-1) + \dot{r}(k)\,\Delta t + p_r\big(\alpha(k) - \dot{r}(k)\big)\Delta t^2$$

with p_u, p_r denoting control gains regulating how fast we require the platform accelerations to converge to the optimal references.

IV. Validation

A. Numerical Simulation

The transition from the mathematical analysis of the path-following controller to the actual ASV kinematics is implemented using the Project11 backseat driver.[2] The controller (13) was first tested on the Project11 simulator (Fig. 4), and its performance was assessed by comparing it with earlier survey navigation and control designs (cf. [1]). The reason for this choice was because the earlier controller design [1] had already been benchmarked against the default Project11 controller, and the interest here is to see how the drift-aware controller design fares compared to its drift-agnostic counterpart.

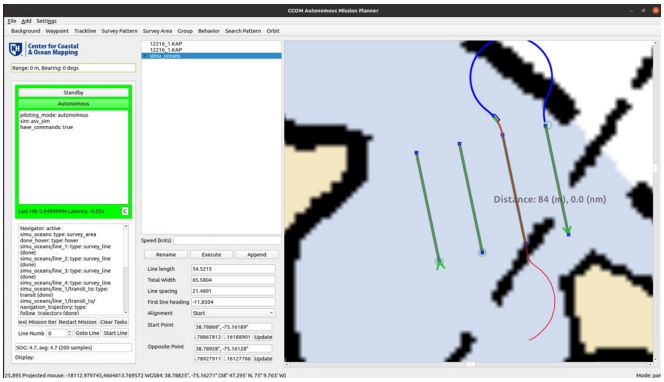

Fig. 4: Screenshot of Project 11's graphical user interface simulating UD's Hugh R. Sharp Campus boat basin.

The simulation conditions on which the two controllers were tested did not involve any environmental disturbances or other perturbations acting on the vehicle. Figure 5a depicts the cross-track error achieved by the two controllers, while

[2]https://github.com/CCOMJHC/project11

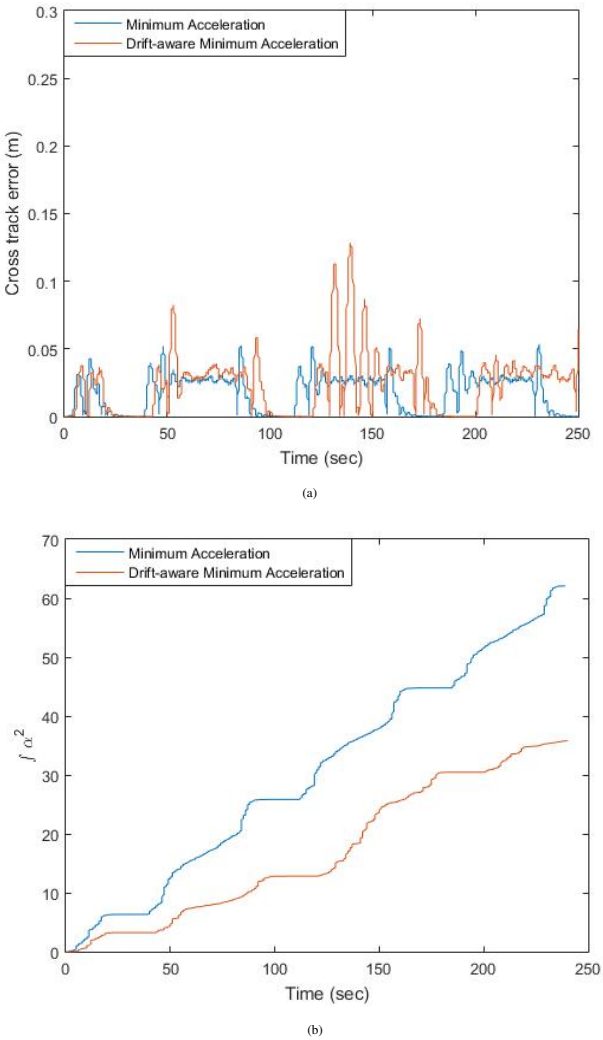

Fig. 5: Motion data from the simulation testing conducted using existing minimum acceleration controller [1] (blue) and the proposed drift-aware minimum acceleration path following controller (red). (a) Cross-track error between the desired trajectory and the actual trajectory. (b) Integral of the yaw accelerations squared over time.

Fig. 5b shows the evolution of the accumulated angular acceleration control effort, which is the input directly associated with the cross-track error output, and which we want to minimize in order to improve sensor data quality. Comparing the responses of the two controllers one observes in Fig. 5a that the cross-track error afforded by the two controllers is comparable (in the order of 5–10 cm) with the drift-aware controller allowing for more error. Figure 5b likely explains the difference since the drift-aware controller utilizes less control effort and therefore induces less lateral motion on the sensor. We expect that the differences seen here in simulation can probably be adjusted to be smaller or bigger depending on the choice of the optimization weight parameter ρ; that said, there will always be a trade-off between actuation effort and cross-tracking error, as seen in Fig. 5.

B. Field Testing

The platform used to test the optimal path-following controller is the Seafloor Systems Echoboat 160 ASV (Fig. 6). The Echoboat 160 is a versatile vehicle primarily used for

shallow water mapping, and it is also a loosely-scaled proxy for larger vehicles used in open water environments. For this study, the vehicle is equipped with a Norbit iWBMSe sonar, georeferenced using navigation data from a POS-MV Surfmaster dual global navigation satellite system (GNSS) aided inertial navigation system (INS). The sonar data, with INS data injected in real-time, are logged using the Norbit GUI and Norbit's Data Collection Tool for real-time quality assurance/quality control (QA/QC). The INS data are also redundantly logged for post-processing. The POS-MV INS data also feed into the ASV's controller.

Fig. 6: The Echoboat 160 ASV, by Seafloor Systems Inc, can serve as an autonomous sensor platform for environmental surveys.

The drift-aware minimum acceleration path-following controller was tested and compared against the previously reported minimum acceleration path-following controller [1] on the Echoboat 160 ASV in short-period chop conditions in the Delaware Bay, DE, USA. These field conditions are roughly equivalent to a Beaufort sea state 3. The testing scenarios involved performing an identical hull-mounted multibeam survey of approximately 0.05 square kilometers with each controller consecutively (total of 2 surveys). The forward speed of the vehicle during both surveys was approximately 1.75 m/s. Each survey duration was approximately 20 minutes, and no appreciable change in wind, waves, or currents occurred between each of the consecutive surveys.

Figure 7 confirms the qualitative observations made in the simulation studies in Fig. 5. In the evolution of the cross-track error of the vessel (Fig. 7a) we see that the cross-track error of the drift-aware controller is about twice that of the drift-agnostic minimum acceleration path tracking controller developed in earlier work [1]. The "pulse-like" nature of the error plots in Fig. 7a reflect the fact that the vessel mostly utilizes its α control input along the straight line segments of the survey path, interspersed with turns connecting the endpoints of parallel segments during which no sensor data is collected. (This pattern can also be observed in Fig. 5 although it is not so prominent.) Consistent with the simulation data of Fig. 5, the integral of the commanded yaw acceleration squared (Fig. 7b) over time showcases the trade-off made between tracking error and actuation effort, with

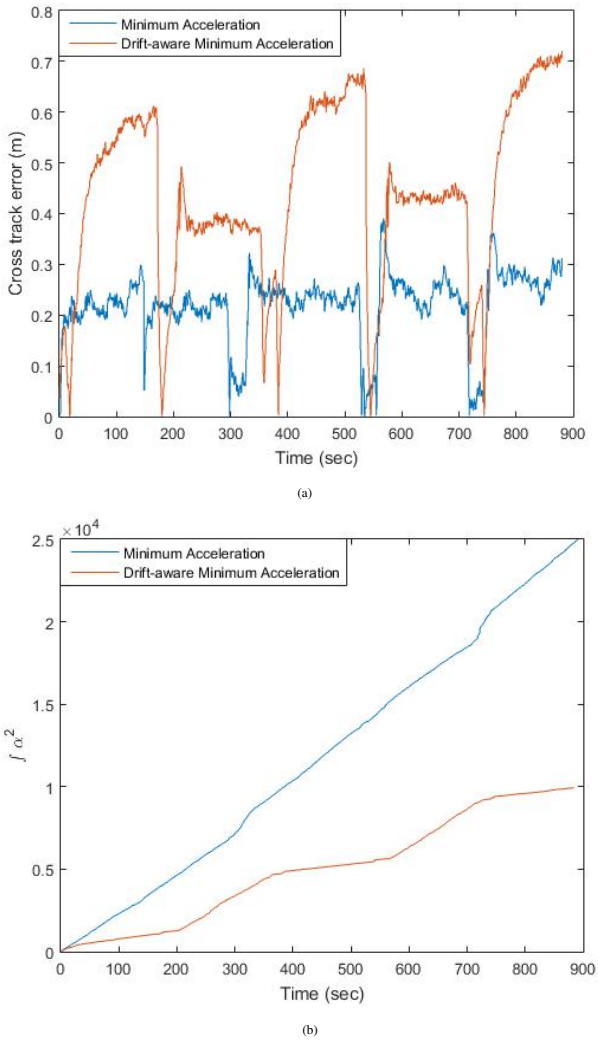

Fig. 7: Motion data from the field testing conducted using existing minimum acceleration controller [1] (blue) and the proposed optimal path following controller (red). (a) Cross-track error between the desired trajectory and the actual trajectory. (b) Integral of the yaw accelerations squared as provided by the INS sensor over time.

the accumulated actuation effort of the drift-aware controller being a little less than half of that used in the drift-agnostic controller.

Each of the two surveys was processed in QPS Qimera by applying sound speed profiles and the multibeam alignment calibration (MAC) (patch test). No automated or manual filtering has been applied to the data; the only data removed were those flagged by the sonar itself for brightness or co-linearity. Surface plots were made for each survey, and three principal metrics are compared: (i) depth/visual artifacts in the end data product, (ii) sounding density, and (iii) 95% uncertainty in the data.

Motion artifacts are clearly identified in both surveys; however, they are far smaller in magnitude and quantity in the drift-aware path-following controller compared to the (drift-agnostic) minimum acceleration controller (Fig. 8). Uncertainty also decreases appreciably (Fig. 10), and although sounding density decreases slightly, it is much more even

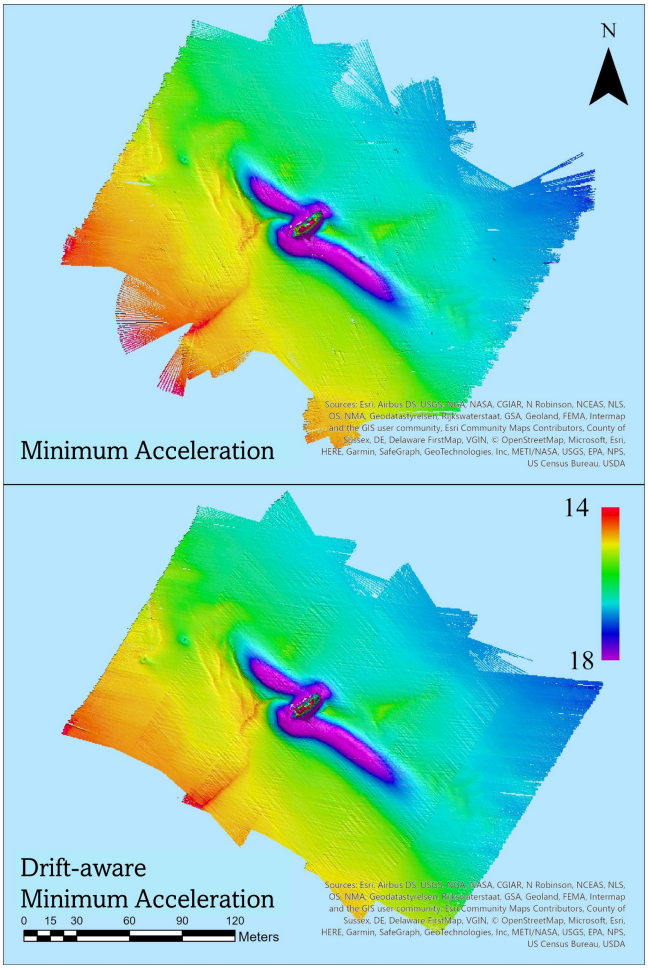

Fig. 8: Bathymetric maps for each controller's survey done in the Delaware Bay. Artifacts are seen in both surveys, but data gaps are decreased in the drift-aware path-following controller survey. Depths are in meters, referenced to the NAVD88 vertical datum.

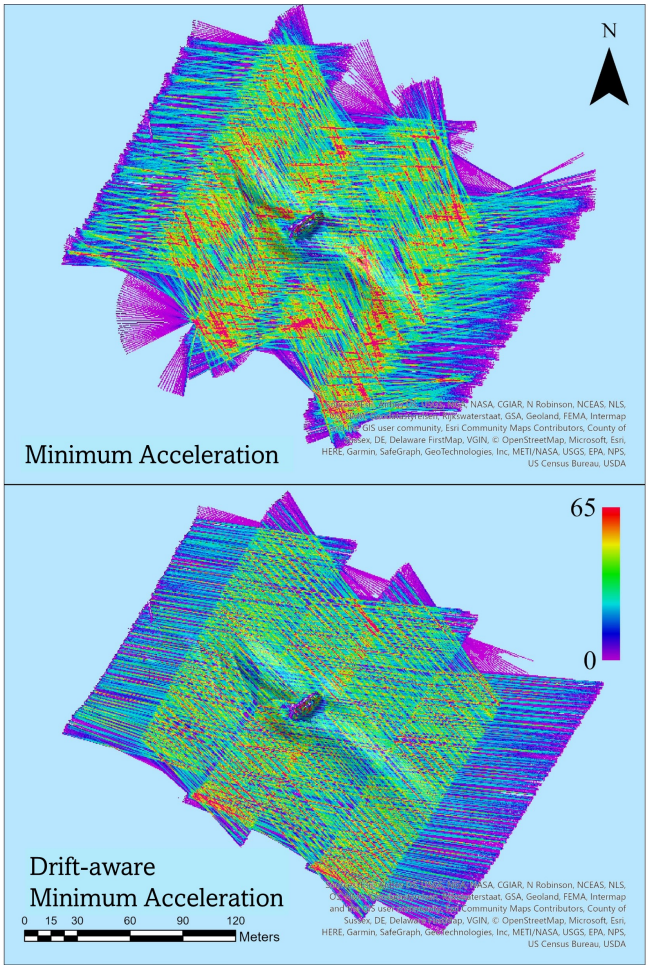

Fig. 9: Sounding density plots for the minimum acceleration and optimal path-following controllers in the Delaware Bay, plotted in soundings per square meter. More even sounding density is seen in the optimal path-following controller's survey.

across the whole map (Fig. 9). Since the minimum sounding density is far more important in the vast majority of mapping efforts than the maximum counterpart, the improvement in sounding density uniformity is seen as a clear indication of the positive impact that the proposed drift-aware path-following controller has on measurement.

V. Conclusion

This work demonstrates the feasibility of development and deployment of an optimal ASV path-following controller that yields minimum linear and angular accelerations at a desired sensor payload location while reacting robustly to sea current forces acting on the vessel. Numerical and field testing confirm its performance compared to existing implementations. Although this controller was tested on a small scale ASV, we do not foresee insurmountable obstacles to implementing and deploying the control design on larger vessels the (3 DOF) kinematics of which are compatible with (1). Benefits of this new control design include more accurate path following during surveying, increased quality of obtained sensor data, and more efficient utilization of onboard power for navigation and control. We expect that these advantages will empower the fast-growing marine robotics scientific community and industry with methodologies and tools for more efficient and effective autonomous surveys.

Acknowledgments

We would like to thank Roland Arsenault and Andy McLeod (University of New Hampshire - Center for Coastal Ocean Mapping) for their help and support in integrating Project11 into our platform. Thanks to Mark Ludine for his assistance with field testing, as well as to Marcos Berrera (Seafloor Systems) and Nick Conway (Norbit Subsea) for their multi-faceted and continuing support.

References

[1] K. Baxevani, G. E. Otto, H. G. Tanner, and A. C. Trembanis, "Development and field testing of an optimal path following asv controller for marine surveys," in *Proceedings of the IEEE/RSJ International Conference on Intelligent Robots and Systems*, 2022, pp. 6861–6866.

[2] B. R. Calder and L. A. Mayer, "Automatic processing of high-rate, high-density multibeam echosounder data," *Geochemistry, Geophysics, Geosystems*, vol. 4, no. 6, 2003.

[3] J. Ghommam, F. Mnif, and N. Derbel, "Global stabilisation and tracking control of underactuated surface vessels," *IET Control Theory & Applications*, vol. 4, no. 1, pp. 71–88, 2010.

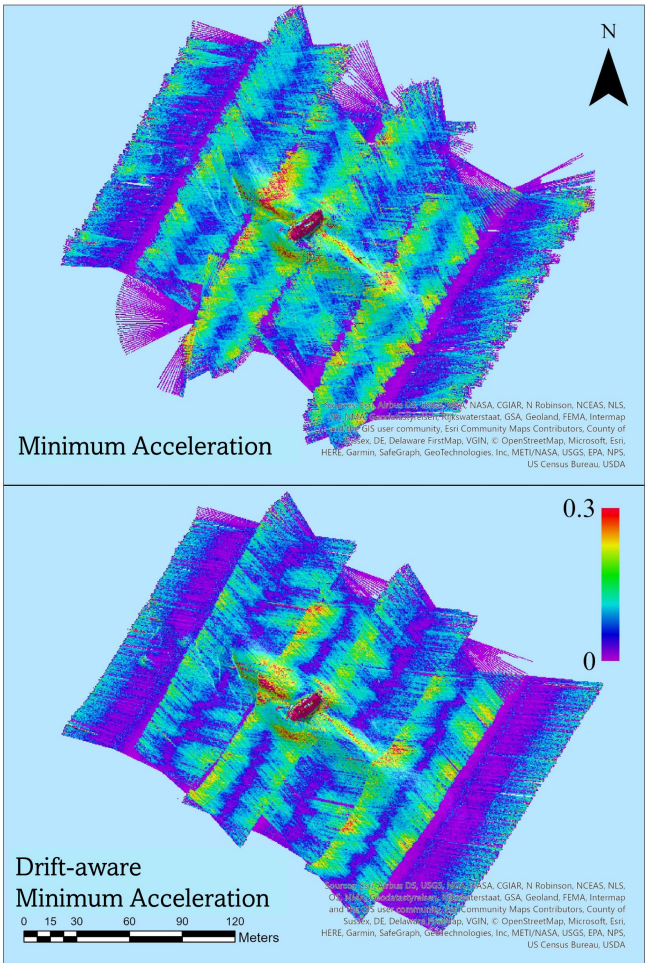

Fig. 10: 95% uncertainty plots for each controller's survey done in the Delaware Bay. Slightly higher uncertainty is seen in the minimum acceleration controller.

[4] Y. Yang, J. Du, H. Liu, C. Guo, and A. Abraham, "A trajectory tracking robust controller of surface vessels with disturbance uncertainties," *IEEE Transactions on Control Systems Technology*, vol. 22, no. 4, pp. 1511–1518, 2013.

[5] Z. Sun, G. Zhang, J. Yang, and W. Zhang, "Research on the sliding mode control for underactuated surface vessels via parameter estimation," *Nonlinear Dynamics*, vol. 91, no. 2, pp. 1163–1175, 2018.

[6] N. Wang, X. Pan, and S.-F. Su, "Finite-time fault-tolerant trajectory tracking control of an autonomous surface vehicle," *Journal of the Franklin Institute*, vol. 357, no. 16, pp. 11 114–11 135, 2020.

[7] C. Liu, R. R. Negenborn, X. Chu, and H. Zheng, "Predictive path following based on adaptive line-of-sight for underactuated autonomous surface vessels," *Journal of Marine Science and Technology*, vol. 23, pp. 483–494, 2018.

[8] Y. Deng and X. Zhang, "Event-triggered composite adaptive fuzzy output-feedback control for path following of autonomous surface vessels," *IEEE Transactions on Fuzzy Systems*, vol. 29, no. 9, pp. 2701–2713, 2020.

[9] Stanford Artificial Intelligence Laboratory et al., "Robotic operating system." [Online]. Available: https://www.ros.org

[10] T. I. Fossen, *Handbook of marine craft hydrodynamics and motion control*. John Wiley & Sons, 2011.

[11] M. Athans and P. L. Falb, *Optimal control : An Introduction to the Theory and its Applications*. McGraw-Hill New York ; Sydney, 1966.